




Article

Predicted Siliconoids by Bridging Si₉ Clusters through sp³-Si Linkers

Laura-Alice Jantke and Thomas F. Fässler * 

Department of Chemistry, Technical University of Munich, Lichtenbergstr. 4, 85747 Garching, Germany;
Laura.Jantke@lrz.tu-muenchen.de

* Correspondence: thomas.faessler@lrz.tum.de

Received: 22 December 2017; Accepted: 17 February 2018; Published: 26 February 2018

Abstract: Charged and neutral silicon clusters comprising Si atoms that are exclusively connected to atoms of the same type serve as models for bulk silicon surfaces. The experimentally known *nido*-[Si₉]^{4−} Zintl cluster is investigated as a building block and allows for a theoretical prediction of novel silicon-rich oligomers and polymers by interconnection of such building units to larger aggregates. The stability and electronic properties of the polymers {¹_∞([Si₉)-(SiCl₂)₂)_n} and {¹_∞([Si₉)-(SiH₂)₂)_n}, as well as of related oligomers are presented.

Keywords: silicon cluster; siliconoid; nanoparticle; computation

1. Introduction

Silicon is the element of choice for fulfilling the desire for novel materials with promising properties. Even though, silicon is an indirect band gap semiconductor resulting in poor efficiency of light emission, the observation of visible photoluminescence from porous silicon or silicon nanoparticles at room temperature reported in the early 90s [1,2] triggered the investigations of low-dimensional silicon quantum structures and had been a subject of extensive investigations due to the potential usage of nano-sized silicon in photonic and optoelectronic devices [3,4].

In recent years, some experimental molecular approaches successfully showed that molecules with low-valent Si atoms can be synthesized. So-called siliconoids [5] are stable unsaturated neutral silicon clusters that show the characteristic structural features of silicon nanoparticles and surfaces in the molecular regime generally realized through the occurrence of one or more unsubstituted Si atoms [5–8].

Computationally, many novel well-ordered Si allotropes of various dimensionality have been proposed [9,10], but only a few of those were experimentally verified, such as the low-density Si allotropes [11] with clathrate-type structures [12–19]. The focus of the research lies on the description, understanding, and discovery of well-performing photovoltaic materials as well as models for bulk silicon surfaces [20,21]. A few such predicted materials are realizable in laboratory to date also applying physical methods such as ultrafast laser-induced confined microexplosion [22].

Currently, one of the most investigated two-dimensional materials is silicene [23], the higher homologue of graphene [24]. It is reported as a buckled sheet of sp³/sp²-hybridized Si atoms connected to wrinkled six membered rings, which is stabilized through intrinsic van-der-Waals interactions [25]. Silicene is experimentally accessible only on metal surfaces [26–28]. Theoretical investigations on this material are reviewed in several articles [29–31]. Another two-dimensional Si modification results from adding ad-atoms to silicene. Si in this MoS₂-structure type shows a lower relative energy compared to silicene [32]. In our recent work, we introduced two-dimensional materials, which may overcome surface reconstruction problems by using {Si₉} Zintl cages (Figure 1a) that are stable in solution [33].

Our aim is the computational investigation using substructures or molecular building units that are experimentally known, which we call the *chemi-inspired* attempt [9,10]. We found that Zintl clusters

of Group 14 elements, as they occur in neat binary intermetallic solids (Zintl phases) [34], represent ideal candidates for constructing tailor-made materials. They have well-defined structures, which are retained upon solvation, and can thus be functionalized, oligomerized, or even polymerized [35,36]. Best suited for such chemistry is the nine-atomic $[E_9]^{(2-4)-}$ cluster ($E = \text{Si, Ge, Sn, and Pb}$). For silicon, only a few examples of following-up reactions of Si_9 clusters are known whereas the pure clusters are structurally characterized in solids [37] and in salts obtained from solution [38–42]. In all examples, reactions occur via atoms of the open square of the mono-capped square antiprism of the *nido*- $[\text{Si}_9]^{4-}$ cluster (Figure 1a); either capped in a η^4 -coordination with phenylzinc (Figure 1b) [39] as well as Cu-NHC (NHC = *N*-heterocyclic carbene) [43] or two clusters are bridged by $\text{Ni}(\text{CO})_2$ fragments via two neighboring atoms of the open square, each involved in a η^1 -coordination (Figure 1c) [40,44].

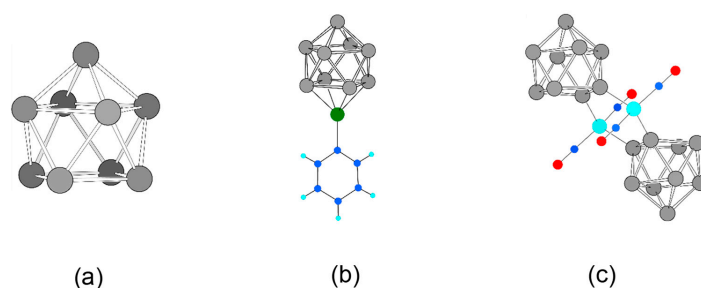


Figure 1. The building block *nido*- $[\text{Si}_9]^{4-}$ and its experimentally accessible complexes from solution. (a) *nido*- $[\text{Si}_9]^{4-}$ optimized on a DFT-PBE0/def2-TZVPP/PCM level of theory; (b) *closo*- $[\text{Si}_9\text{Zn}(\text{C}_6\text{H}_5)]^{3-}$ [39]; (c) $[\text{Ni}(\text{CO})_2]_2(\mu\text{-Si}_9)_2^{8-}$ [40,44]. Si, C, H, Zn, Ni, and O are shown as grey, blue, light blue, green, turquoise, and red spheres.

Further, it was shown that such clusters can serve as seed crystals for the synthesis of Si nanoparticles and nanoscale materials [45,46]. In analogy to Ge_9 clusters for which covalently bonded Ge_9 oligomers and polymers are experimentally known, Si-based materials that contain Si_9 units linked via the atoms of the open square are feasible [39,41,44]. The direct linkage has already been discussed and also the stability and properties of two-dimensional Si materials containing sp^3 -hybridized Si atoms as linkers between Si_9 clusters were computationally investigated [33]. In this work, we explore the possibilities of introducing tetrahedrally connecting sp^3 -Si atoms, which might occur from a formal reaction of the anions with SiCl_4 and SiH_2Cl_2 and *nido*- $[\text{Si}_9]^{4-}$ clusters. Thus, we investigate the complexes $[\text{Si}(\text{Si}_9)\text{Cl}_3]^{3-}$ and $[\text{Si}(\text{Si}_9)\text{Me}_3]^{3-}$ ($\text{Me} = -\text{CH}_3$), $[\text{Si}(\text{Si}_9)_2\text{Cl}_2]^{6-}$, $[\text{Si}(\text{Si}_9)_3\text{Cl}]^{9-}$, and $[\text{Si}(\text{Si}_9)_4]^{12-}$. Further, we analyze the hypothetical insertion of *nido*- $[\text{Si}_9]^{4-}$ clusters into polysilanes resulting in the neutral polymers $\{^1_\infty([\text{Si}_9]-(\text{SiCl}_2)_2)_n\}$ and $\{^1_\infty([\text{Si}_9]-(\text{SiH}_2)_2)_n\}$.

2. Computational Details

Neutral polymers containing silane fragments and Si_9 clusters as well as the polysilanes themselves were optimized starting from manually drawn structures pre-optimized using UFF [47,48]. The lattice and atomic positions were allowed to relax during optimization within the constraints given by rod group symmetry [49]. All quantum chemical calculations for the polymers were carried out using the CRYSTAL09 program package [50] with a hybrid DFT functional after Perdew, Burke, and Ernzerhof (DFT-PBE0) [51,52]. For silicon, a modified split-valence + polarization (SVP) basis set [53] was applied. The shrinking factor (SHRINK) for generating the Monkhorst-Pack-type grid of k points in the reciprocal space was set to 4, resulting in three k -points in the irreducible Brillouin zone. For the evaluation of the Coulomb and exchange integrals tight tolerance factors (TOLINTEG) of 8, 8, 8, 8, and 16 were chosen. Default optimization convergence thresholds and an extra-large integration grid (XLGRID) for the density-functional part were applied in all calculations. Harmonic vibrational frequencies were calculated numerically to confirm the stationary point on the potential-energy surface as a true minimum.

The investigations on charged complexes containing *nido*-[Si₉]^{4−} as a building block are done with the DFT-PBE0 [51,52] hybrid DFT functional and def2-TVZPP level basis sets for the elements Si, Cl, H, and C using the Gaussian09 program package [54]. For modelling a solvation effect, a solvation model (polarizable continuum model, PCM) with standard settings was applied [55]. For structure optimizations, extremely tight optimization convergence criteria were combined with a large and ultrafine DFT integration grid. The systems were allowed to relax without symmetry restrictions. Harmonic vibrational frequencies were calculated analytically to confirm the stationary point on the potential-energy surface as a true minimum (except for **M6**).

The position parameters for all optimized compounds are listed in the Supplementary Materials.

3. Results and Discussion

3.1. Neutral Polymers with SiCl₂ or SiH₂ Linkers between the Clusters

Inspired by the [(Ni(CO)₂)₂(μ-Si₉)₂]^{8−} complex [40,44] (Figure 1c) and in continuation of our work on 2D structures containing Si₉ clusters [33], we derived two polymers {¹_∞[(Si₉)-(SiCl₂)₂]_n} (**P1**) and {¹_∞[(Si₉)-(SiH₂)₂]_n} (**P2**) by a formal replacement of Ni(CO)₂ with isolobal SiCl₂ or SiH₂. The polymers can also be regarded as silanes with inserting Si₉ units. Pauling electronegativity of Ni and Si are almost identical with a value of χ_{Ni} = 1.91 and χ_{Si} = 1.90, respectively, and the electron withdrawing effect of the CO ligands is considered by choosing ligands whose electronegativity is higher if compared to Si (χ_{Cl} = 3.16 and χ_H = 2.20).

The energetically optimized polymers **P1** and **P2** possess nearly ideal C_{4v} symmetric Si₉ units in the rod group *pmn*2 (relevant bond lengths are listed in Table S1, Supplementary Materials). The two bridging Si atoms and two adjacent atoms of each of the two open squares form a planar hexagon which is compressed along the propagation direction of the polymer. The bond angles at the bridging Si atom consequently lie in the range of tetrahedral angles 103.4°–111.0° for both compounds. The torsional angles between these hexagons and the open square of the *nido*-clusters are 165.8° and 160.3° for **P1** and **P2**, respectively. In order to compare the total energy with respect to α-Si and since the compounds contain also X = H and Cl atoms we include polysilanes with comparable bond situations according to Equation (1):

$$\Delta E_{\text{rel}}(^1_{\infty}[\text{Si}_9-(\text{SiX}_2)_2]) = \Delta E_{\text{tot}}(^1_{\infty}[\text{Si}_9-(\text{SiX}_2)_2]) - [9 \cdot E_{\text{tot}}(\alpha\text{-Si}) + 2 \cdot E_{\text{tot}}(^1_{\infty}[\text{SiX}_2])] \quad (1)$$

The resulting values of 7.28 eV and 7.23 eV for X = Cl and H, respectively refer to one formula unit (Si₉)(SiX₂)₂ (X = Cl, H) for **P1** and for **P2**, respectively (Figure 2). Scaled to one Si atom per formula unit these values result in 0.56 eV for both compounds. On a first glance, the values seem high if compared to α-Si, however the polymers must rather be compared to Si nanoparticles than to bulk materials. In this context the values are rather close to the relative energy of the carbon fullerenes of which for example C₆₀ which is 0.48 eV per atom higher in total energy than diamond [56]. The Si bridged clusters are also much lower in energy than the directly connected clusters (0.96 eV) [33]. Energetically, the differences between Si–Cl and Si–H bonds are negligible.

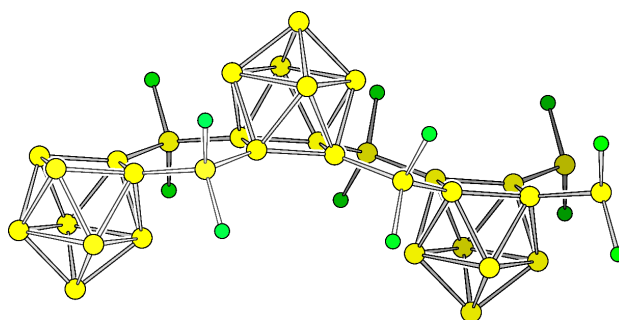


Figure 2. Cut-out of polymer **P1**. Si and Cl are shown as yellow and green spheres, respectively.

3.2. Charged Molecules—The Stepwise Ligand Exchange in SiCl_4 to $[\text{Si}_{17}]^{12-}$

Siliconoid molecules are formed by a stepwise substitution of heteroatomic bonds between ligands bound to a central Si atom with Si terminated groups. We computationally substituted ligands in SiX_4 by $[\text{Si}_9]^{4-}$ for $\text{X} = \text{Cl}, \text{H}$, and CH_3 . The resulting molecular ions $[\text{Si}(\text{Si}_9)\text{Cl}_3]^{3-}$ (**M1**), $[\text{Si}(\text{Si}_9)\text{H}_3]^{3-}$ (**M2**) and $[\text{Si}(\text{Si}_9)\text{Me}_3]^{3-}$ (**M3**) differ in the ligands at the sp^3 -Si atom (Table 1). We started the optimizations for all compounds from a η^1 -connected isomer with an ideal C_{4v} symmetric *nido*- $[\text{Si}_9]^{4-}$ cluster.

As the energetically most favorite structure of **M1** we found an arrangement with an almost perfect D_{3h} symmetric trigonal prismatic Si_9 cluster with the SiCl_3 group symmetrically capping a triangular face of the Si_9 cluster. The three distances between the Si atoms of the SiCl_3 group and the Si atoms of the clusters are with a value of 2.58 Å identical to the lengths of the triangular face of Si_9 , consequently forming an almost undistorted tetrahedron. The three Si–Cl distances are 2.20 Å. The shape of Si_9 cluster distorts to a tricapped trigonal prism with prism heights of 2.69 Å that are elongated with respect to the triangular faces. The opposing trigonal face, which is not capped, has considerable shorter lengths edges of 2.46 Å and 2.49 Å. Thus the coordination of the SiCl_3 group leads to an elongation of edges of the capped triangle.

Interestingly, no local minimum structure with η^1 -coordination of the SiCl_3 groups were found. In contrast, for $[\text{Si}(\text{Si}_9)\text{H}_3]^{3-}$ (**M2**) and $[\text{Si}(\text{Si}_9)\text{Me}_3]^{3-}$ (**M3**) the energetically most favored structures remain with η^1 -coordinated Si_9 clusters. For both anions, the Si_9 clusters distort to (pseudo)- C_{2v} symmetric cages as an intermediate of the mono-capped square anti prism and the tricapped trigonal prism. With the ratio of diagonal lengths of the open square of $d_1/d_2 = 1.22$ is **M2** more distorted than **M3** ($d_1/d_2 = 1.16$). The bond length between the clusters and their ligands are 2.33 Å and 2.35 Å, respectively. The prism heights are 2.63 Å, 2.64 Å, and 3.08 Å for **M2** and 2.62 Å, 2.63 Å, and 3.18 Å for **M3**.

Bridging two clusters by a single SiCl_2 fragment, e.g. attaching two clusters to one central Si atom leads to the anion of composition $[\text{SiCl}_2(\text{Si}_9)_2]^{6-}$ (**M4**). Both Si_9 clusters in **M4** form a η^1 -coordination with distances between the cluster and the bridge atoms of 2.34 Å. The Si–Cl bonds of 2.13 Å and 2.14 Å are shorter than for **M1**. Both clusters within **M4** deform after optimization to (pseudo)- C_{2v} symmetric compounds with $d_1/d_2 = 1.21$ and 1.22. (The distortion of C_{4v} symmetric monocapped square anti prism can be characterized by the ratio of the diagonal lengths d_1 and d_2 of the open square. For an undistorted cage the ratio is equal to 1. Deviation from this ratio leads to cages with C_{2v} symmetry.) The bond angle between the central Si atom and the two bonded Si atoms of the clusters is 121.7° and thus larger than the tetrahedral angle, which is most probably due to the steric demands of the Si_9 ligands.

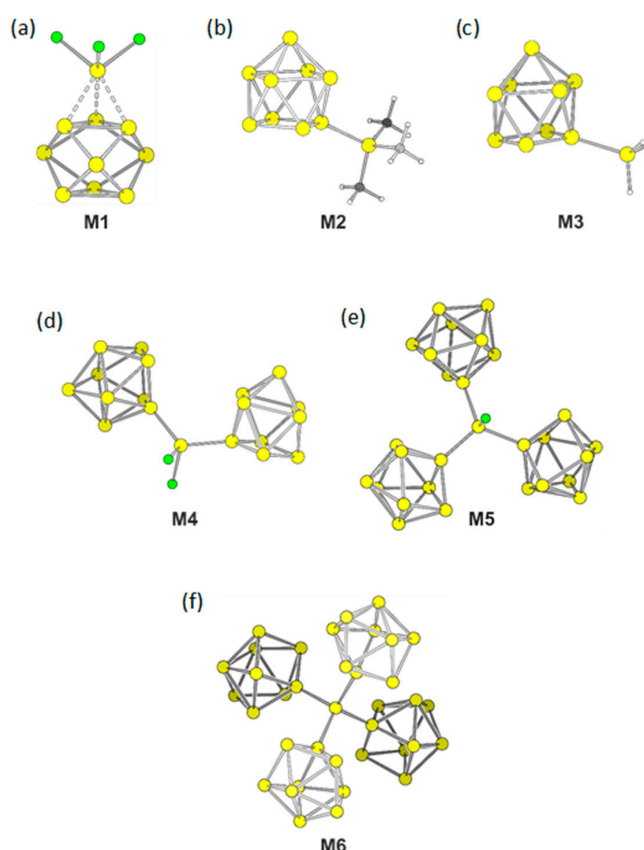
Substitution of another Cl ligand by a third $[\text{Si}_9]^{4-}$ results in the highly charged cluster $[\text{SiCl}(\text{Si}_9)_3]^{9-}$ (**M5**). In **M5** the three (pseudo)- C_{2v} symmetric clusters have diagonal length ratio in the narrow range of $d_1/d_2 = 1.15$ –1.17 and bond lengths of 2.37 Å between cluster atoms and the central sp^3 -Si atom for each bond. The distance Si–Cl is 1.18 Å.

A replacement of all Cl ligands by Si_9 units results in $[\text{Si}(\text{Si}_9)_4]^{12-}$ (**M6**). Such highly charged clusters are not unrealistic, since a salt containing a $[\text{Ge}_{45}]^{12-}$ cluster unit, which is attached to three Au^+ ions ($[\text{Au}_3\text{Ge}_{45}]^{9-}$) had been isolated and structurally characterized [57]. The distances for all four Si–Si bonds at the central Si atom are 2.39 Å. The angles range between 105.1° and 117.3° . The clusters are again distorted towards C_{2v} symmetric cages, but stay close to the C_{4v} symmetric input with ratios of the diagonal lengths of the open square between $d_1/d_2 = 1.11$ –1.15. A table listing all bond distances and relevant cluster parameters is located in the Supplementary Materials.

The building unit **M6** can be extended by continuation the building scheme with more SiCl_4 . Successive linking $[\text{Si}_9]^{4-}$ clusters with SiCl_4 under Cl substitution results in a neutral two-dimensional $\infty^2\{[(\text{Si}_9)\text{--Si}]_n\}$ sheet [33].

Table 1. Structural analysis of molecular anions (Figure 3). All values are averaged, if more bonds or angles of the same type exist.

Molecular Anions	Distances/Å	Distances/Å	Angles/°	Angles/°	Angles/°
	X ₃ Si–Si(Si ₉)	Si–Cl	X–Si–X	(Si ₉)–Si–X	(Si ₉)–Si–(Si ₉)
M1	2.58 (η^3)	2.20	94.6	-	-
M2	2.33	-	105.3	113.3	-
M3	2.35	-	107.8	111.1	-
M4	2.34	2.14	101.2	107.9	121.7
M5	2.37	2.18	-	100.6	116.7
M6	2.39	-	-	-	109.4

**Figure 3.** Optimized structures of molecular anions **M1–M6**. (a) η^3 -[Si(Si₉)Cl₃]^{3−} (**M1**), (b) η^1 -[Si(Si₉)Me₃]^{3−} (**M2**), (c) η^1 -[Si(Si₉)H₃]^{3−} (**M3**), (d) [SiCl₂(Si₉)₂]^{6−} (**M4**), (e) [SiCl(Si₉)₃]^{9−} (**M5**), (f) [Si(Si₉)₄]^{12−} (**M6**). Si and Cl atoms are shown as yellow and green spheres, respectively.

4. Conclusion

The modelling of polymeric Si₉ chains gave interesting insights to the chemistry of this up to now hard to functionalize Si₉ cluster. It showed that a replacement of Ni(CO)₂ as a ligand by others bridging sp³-Si units with comparable electron withdrawing effects, namely SiH₂ and SiCl₂, leads to polymers that are energetically in a range for realizable materials. The formation of charged oligomers by the formal substitution of X ligands in SiX₄ by [Si₉]^{4−} clusters leads to stable anions [SiCl_{4−x}(Si₉)_x]^{3x−}. For all derivatives, stable anions with covalent Si–Si bonds to the central Si atom form, except for x = 1 and X = Cl. Here, a η^3 -coordination of the cluster to the Si atom of the SiCl₃ group is observed. Whereas the monomeric unit [Si(Si₉)₄]^{12−} (**M6**) possesses a relative high charge, further combination with bridging Si atoms leads to a relatively stable two-dimensional neutral Si allotrope.

Supplementary Materials: The following are available online at www.mdpi.com/2304-6740/6/1/31/s1, Bond lengths for Si₉ clusters within the different compounds; Band Structures and DOSs of Polymers; Position Parameters for Polymers; Vibrational Frequencies for Polymers; Position Parameters for Molecular Compounds; Vibrational Frequencies of Molecular Compounds.

Acknowledgments: The authors are grateful to the SolTech (Solar Technologies go Hybrid) program of the Bavarian State Ministry of Education, Science and the Arts for financial support.

Author Contributions: Laura-Alice Jantke and Thomas F. Fässler conceived and designed the structures. Laura-Alice Jantke performed all quantum chemical calculations, Laura-Alice Jantke and Thomas F. Fässler wrote and corrected the paper, respectively.

Conflicts of Interest: The authors declare no conflict of interest.

References

1. Cullis, A.G.; Canham, L.T. Visible light emission due to quantum size effects in highly porous crystalline silicon. *Nature* **1991**, *353*, 335–338. [[CrossRef](#)]
2. Canham, L.T. Silicon quantum wire array fabrication by electrochemical and chemical dissolution of wafers. *Appl. Phys. Lett.* **1990**, *57*, 1046–1048. [[CrossRef](#)]
3. Bisi, O.; Ossicini, S.; Pavesi, L. Porous silicon: A quantum sponge structure for silicon based optoelectronics. *Surf. Sci. Rep.* **2000**, *38*, 1–126. [[CrossRef](#)]
4. Geppert, T.; Schiling, J.; Wehrspohn, R.; Gösele, U. Silicon-based photonic crystals. In *Silicon Photonics*; Pavesi, L., Lockwood, D.J., Eds.; Springer: Berlin, Germany, 2004; Volume 94, pp. 295–322. ISBN 978-3-540-21022-1.
5. Abersfelder, K.; Russell, A.; Rzepa, H.S.; White, A.J.; Haycock, P.R.; Scheschkewitz, D. Contraction and expansion of the silicon scaffold of stable Si₆R₆ isomers. *J. Am. Chem. Soc.* **2012**, *134*, 16008–16016. [[CrossRef](#)] [[PubMed](#)]
6. Iwamoto, T.; Akasaka, N.; Ishida, S. A heavy analogue of the smallest bridgehead alkene stabilized by a base. *Nat. Commun.* **2014**, *5*, 5353. [[CrossRef](#)] [[PubMed](#)]
7. Abersfelder, K.; White, A.J.; Rzepa, H.S.; Scheschkewitz, D. A tricyclic aromatic isomer of hexasilabenzene. *Science* **2010**, *327*, 564–566. [[CrossRef](#)] [[PubMed](#)]
8. Scheschkewitz, D. A molecular silicon cluster with a “naked” vertex atom. *Angew. Chem. Int. Ed.* **2005**, *44*, 2954–2956. [[CrossRef](#)] [[PubMed](#)]
9. Jantke, L.A.; Stegmaier, S.; Karttunen, A.J.; Fässler, T.F. Slicing Diamond—A Guide to Deriving sp³-Si Allotropes. *Chem. Eur. J.* **2017**, *23*, 2734–2747. [[CrossRef](#)] [[PubMed](#)]
10. Jantke, L.A.; Karttunen, A.J.; Fässler, T.F. Slicing Diamond for More sp³-Group 14 Allotropes Ranging from Direct Bandgaps to Poor Metals. *ChemPhysChem* **2017**, *18*, 1992–2006. [[CrossRef](#)] [[PubMed](#)]
11. Beekman, M.; Wei, K.; Nolas, G.S. Clathrates and beyond: Low-density allotropy in crystalline silicon. *Appl. Phys. Rev.* **2016**, *3*, 040804. [[CrossRef](#)]
12. O’Keeffe, M.; Adams, G.B.; Sankey, O.F. Duals of Frank-Kasper structures as C, Si and Ge clathrates: Energetics and structure. *Philosoph. Mag. Lett.* **1998**, *78*, 21–28. [[CrossRef](#)]
13. Krishna, L.; Martinez, A.D.; Baranowski, L.L.; Brawand, N.P.; Koh, C.A.; Stevanovic, V.; Lusk, M.T.; Toberer, E.S.; Tamboli, A.C. Group IV clathrates: Synthesis, optoelectronic properties, and photovoltaic applications. *Proceedings* **2014**, *8981*, 898108.
14. Norouzzadeh, P.; Myles, C.W.; Vashae, D. Prediction of Giant Thermoelectric Power Factor in Type-VIII Clathrate Si₄₆. *Sci. Rep.* **2014**, *4*, 7028. [[CrossRef](#)] [[PubMed](#)]
15. Härkönen, V.J.; Karttunen, A.J. Ab initio studies on the lattice thermal conductivity of silicon clathrate frameworks II and VIII. *Phys. Rev. B* **2016**, *93*, 024307. [[CrossRef](#)]
16. Ammar, A.; Cros, C.; Pouchard, M.; Jaussaud, N.; Bassat, J.-M.; Villeneuve, G.; Duttine, M.; Ménétrier, M.; Reny, E. On the clathrate form of elemental silicon, Si₁₃₆: Preparation and characterisation of Na_xSi₁₃₆ (x→0). *Solid State Sci.* **2004**, *6*, 393–400. [[CrossRef](#)]
17. Ohashi, F.; Hattori, M.; Ogura, T.; Koketsu, Y.; Himeno, R.; Kume, T.; Ban, T.; Iida, T.; Habuchi, H.; Natsuhara, H.; et al. High-yield synthesis of semiconductive type-II Si clathrates with low Na content. *J. Non-Cryst. Solids* **2012**, *358*, 2134–2137. [[CrossRef](#)]
18. Baranowski, L.L.; Krishna, L.; Martinez, A.D.; Raharjo, T.; Stevanovic, V.; Tamboli, A.C.; Toberer, E.S. Synthesis and optical band gaps of alloyed Si–Ge type II clathrates. *J. Mater. Chem. C* **2014**, *2*, 3231–3237. [[CrossRef](#)]

19. Krishna, L.; Baranowski, L.L.; Martinez, A.D.; Koh, C.A.; Taylor, P.C.; Tamboli, A.C.; Toberer, E.S. Efficient route to phase selective synthesis of type II silicon clathrates with low sodium occupancy. *Cryst. Eng. Comm* **2014**, *16*, 3940–3949. [[CrossRef](#)]
20. Buriak, J.M. Organometallic Chemistry on Silicon and Germanium Surfaces. *Chem. Rev.* **2002**, *102*, 1271–1308. [[CrossRef](#)] [[PubMed](#)]
21. Wippermann, S.; He, Y.P.; Voros, M.; Galli, G. Novel silicon phases and nanostructures for solar energy conversion. *Appl. Phys. Rev.* **2016**, *3*, 040807. [[CrossRef](#)]
22. Rapp, L.; Haberl, B.; Pickard, C.J.; Bradby, J.E.; Gamaly, E.G.; Williams, J.S.; Rode, A.V. Experimental evidence of new tetragonal polymorphs of silicon formed through ultrafast laser-induced confined microexplosion. *Nat. Commun.* **2015**, *6*, 7555. [[CrossRef](#)] [[PubMed](#)]
23. Guzmán-Verri, G.G.; Lew Yan Voon, L.C. Electronic structure of silicon-based nanostructures. *Phys. Rev. B* **2007**, *76*, 075131. [[CrossRef](#)]
24. Novoselov, K.S.; Geim, A.K.; Morozov, S.V.; Jiang, D.; Zhang, Y.; Dubonos, S.V.; Grigorieva, I.V.; Firsov, A.A. Electric Field Effect in Atomically Thin Carbon Films. *Science* **2004**, *306*, 666–669. [[CrossRef](#)] [[PubMed](#)]
25. Cahangirov, S.; Topsakal, M.; Akturk, E.; Sahin, H.; Ciraci, S. Two- and one-dimensional honeycomb structures of silicon and germanium. *Phys. Rev. Lett.* **2009**, *102*, 236804. [[CrossRef](#)] [[PubMed](#)]
26. Lin, C.-L.; Arafune, R.; Kawahara, K.; Tsukahara, N.; Minamitani, E.; Kim, Y.; Takagi, N.; Kawai, M. Structure of Silicene Grown on Ag(111). *Appl. Phys. Express* **2012**, *5*, 045802. [[CrossRef](#)]
27. Fleurence, A.; Friedlein, R.; Ozaki, T.; Kawai, H.; Wang, Y.; Yamada-Takamura, Y. Experimental evidence for epitaxial silicene on diboride thin films. *Phys. Rev. Lett.* **2012**, *108*, 245501. [[CrossRef](#)] [[PubMed](#)]
28. Meng, L.; Wang, Y.; Zhang, L.; Du, S.; Wu, R.; Li, L.; Zhang, Y.; Li, G.; Zhou, H.; Hofer, W.A.; et al. Buckled Silicene Formation on Ir(111). *Nano Lett.* **2013**, *13*, 685–690. [[CrossRef](#)] [[PubMed](#)]
29. Zhuang, J.; Xu, X.; Feng, H.; Li, Z.; Wang, X.; Du, Y. Honeycomb silicon: A review of silicene. *Sci. Bull.* **2015**, *60*, 1551–1562. [[CrossRef](#)]
30. Kaloni, T.P.; Schreckenbach, G.; Freund, M.S.; Schwingenschlögl, U. Current developments in silicene and germanene. *Phys. Status Solidi RRL* **2016**, *10*, 133–142. [[CrossRef](#)]
31. Voon, L.C.L.Y.; Zhu, J.; Schwingenschlögl, U. Silicene: Recent theoretical advances. *Appl. Phys. Rev.* **2016**, *3*, 040802. [[CrossRef](#)]
32. Gimbert, F.; Lee, C.-C.; Friedlein, R.; Fleurence, A.; Yamada-Takamura, Y.; Ozaki, T. Diverse forms of bonding in two-dimensional Si allotropes: Nematic orbitals in the MoS₂ structure. *Phys. Rev. B* **2014**, *90*, 165423. [[CrossRef](#)]
33. Jantke, L.-A.; Karttunen, A.J.; Fässler, T.F. Chemi-inspired silicon allotropes—Experimentally accessible Si₉ cages as building block for 1D polymers, 2D sheets, single-walled nanotubes, and nanoparticles, submitted.
34. Fässler, T.F. Zintl phases: Principles and recent developments. In *Structure and Bonding*; Mingos, D.M.P., Ed.; Springer: Heidelberg, Germany, 2011; Volume 139, ISBN 978-3-642-21150-8.
35. Scharfe, S.; Kraus, F.; Stegmaier, S.; Schier, A.; Fässler, T.F. Zintl Ions, Cage Compounds, and Intermetalloid Clusters of Group 14 and Group 15 Elements. *Angew. Chem. Int. Ed.* **2011**, *50*, 3630–3670. [[CrossRef](#)] [[PubMed](#)]
36. Fässler, T.F. Zintl ions: Principles and recent developments. In *Structure and Bonding*; Mingos, D.M.P., Ed.; Springer: Heidelberg, Germany, 2011; Volume 140, ISBN 978-3-642-21181-2.
37. Queneau, V.; Todorov, E.; Sevov, S.C. Synthesis and structure of isolated silicon clusters of nine atoms. *J. Am. Chem. Soc.* **1998**, *120*, 3263–3264. [[CrossRef](#)]
38. Goicoechea, J.M.; Sevov, S.C. Ligand-free deltahedral clusters of silicon in solution: Synthesis, structure, and electrochemistry of [Si₉]^{2−}. *Inorganic Chemistry* **2005**, *44*, 2654–2658. [[CrossRef](#)] [[PubMed](#)]
39. Goicoechea, J.M.; Sevov, S.C. Organozinc derivatives of deltahedral zintl ions: Synthesis and characterization of closo-[E₉Zn(C₆H₅)₃]^{3−} (E = Si, Ge, Sn, Pb). *Organometallics* **2006**, *25*, 4530–4536. [[CrossRef](#)]
40. Joseph, S.; Hamberger, M.; Mutzbauer, F.; Härtl, O.; Meier, M.; Korber, N. Chemistry with Bare Silicon Clusters in Solution: A Transition-Metal Complex of a Polysilicide. *Anion Angew. Chem. Int. Ed.* **2009**, *48*, 8770–8772. [[CrossRef](#)] [[PubMed](#)]
41. Joseph, S.; Suchentrunk, C.; Kraus, F.; Korber, N. [Si₉]^{4−} Anions in Solution—Structures of the Solvates Rb₄Si₉·4.75NH₃ and [Rb(18-crown-6)]Rb₃Si₉·4NH₃, and Chemical Bonding in [Si₉]^{4−}. *Eur. J. Inorg. Chem.* **2009**, *2009*, 4641–4647. [[CrossRef](#)]

42. Waibel, M.; Kraus, F.; Scharfe, S.; Wahl, B.; Fässler, T.F. $[(\text{MesCu})_2(\eta^3\text{-Si}_4)]^{4-}$: A Mesitylcopper-Stabilized Tetrasilicide Tetraanion. *Angew. Chem. Int. Ed.* **2010**, *49*, 6611–6615. [[CrossRef](#)] [[PubMed](#)]
43. Geitner, F.S.; Fässler, T.F. Low Oxidation State Silicon Clusters—Synthesis and Structure of $[\text{NHCDippCu}(\eta^4\text{-Si}_9)]^{2-}$. *Chem. Commun.* **2017**, *53*, 12974–12977. [[CrossRef](#)] [[PubMed](#)]
44. Gärtner, S.; Hamberger, M.; Korber, N. The First Chelate-Free Crystal Structure of a Silicide Transition Metal Complex $\text{K}_{0.28}\text{Rb}_{7.72}\text{Si}_9(\text{Ni}(\text{CO})_2)_2 \cdot 16\text{NH}_3$. *Crystals* **2015**, *5*, 275–282. [[CrossRef](#)]
45. Riley, A.E.; Korlann, S.D.; Richman, E.K.; Tolbert, S.H. Synthesis of semiconducting thin films with nanometer-scale periodicity by solution-phase coassembly of zintl clusters with surfactants. *Angew. Chem. Int. Ed.* **2005**, *45*, 235–241. [[CrossRef](#)] [[PubMed](#)]
46. Nolan, B.M.; Henneberger, T.; Waibel, M.; Fässler, T.F.; Kauzlarich, S.M. Silicon Nanoparticles by the Oxidation of $[\text{Si}_4]^{4-}$ - and $[\text{Si}_9]^{4-}$ - Containing Zintl Phases and Their Corresponding Yield. *Inorg. Chem.* **2015**, *54*, 396–401. [[CrossRef](#)] [[PubMed](#)]
47. Hanson, B. *Jmol: An open-source Java viewer for chemical structures in 3D*; Northfield, MN, USA, 2016.
48. Rappe, A.M.; Joannopoulos, J.D.; Bash, P.A. A test of the utility of plane-waves for the study of molecules from first principles. *J. Am. Chem. Soc.* **1992**, *114*, 6466–6469. [[CrossRef](#)]
49. Dovesi, R.; Saunders, V.R.; Roetti, R.; Orlando, R.; Zicovich-Wilson, C.M.; Pascale, F.; Civalieri, B.; Doll, K.; Harrison, N.M.; Bush, I.J.; et al. *CRYSTAL09 User's Manual*; University of Turino: Turino, Italy, 2009.
50. Dovesi, R.; Orlando, R.; Civalieri, B.; Roetti, C.; Saunders, V.R.; Zicovich-Wilson, C.M. CRYSTAL: A computational tool for the ab initio study of the electronic properties of crystals. *Z. Kristallogr.* **2005**, *220*, 571–573. [[CrossRef](#)]
51. Perdew, J.P.; Burke, K.; Ernzerhof, M. Generalized gradient approximation made simple. *Phys. Rev. Lett.* **1996**, *77*, 3865–3868. [[CrossRef](#)] [[PubMed](#)]
52. Adamo, C.; Barone, V. Toward reliable density functional methods without adjustable parameters: The PBE0 model. *J. Chem. Phys.* **1999**, *110*, 6158–6170. [[CrossRef](#)]
53. Karttunen, A.J.; Fässler, T.F.; Linnolahti, M.; Pakkanen, T.A. Structural Principles of Semiconducting Group 14 Clathrate Frameworks. *Inorg. Chem.* **2011**, *50*, 1733–1742. [[CrossRef](#)] [[PubMed](#)]
54. Frisch, M.J.; Trucks, G.W.; Schlegel, H.B.; Scuseria, G.E.; Robb, M.A.; Cheeseman, J.R.; Scalmani, G.; Barone, V.; Mennucci, B.; Petersson, G.A.; et al. *Gaussian 09*; Gaussian, Inc.: Wallingford, CT, USA, 2009.
55. Scalmani, G.; Frisch, M.J. Continuous surface charge polarizable continuum models of solvation. I. General formalism. *J. Chem. Phys.* **2010**, *132*, 114110. [[CrossRef](#)] [[PubMed](#)]
56. Karttunen, A.J.; Fässler, T.F.; Linnolahti, M.; Pakkanen, T.A. Two-, One-, and Zero-Dimensional Elemental Nanostructures Based on Ge_9 -Clusters. *ChemPhysChem* **2010**, *11*, 1944–1950. [[CrossRef](#)] [[PubMed](#)]
57. Spiekermann, A.; Hoffmann, S.D.; Kraus, F.; Fässler, T.F. $[\text{Au}_3\text{Ge}_{18}]^{5-}$ —A gold-germanium cluster with remarkable Au–Au interactions. *Angew. Chem. Int. Ed.* **2007**, *46*, 1638–1640. [[CrossRef](#)] [[PubMed](#)]

